

Climate Change and Curtailment: Evaluating Water Management Practices in the Context of Changing Runoff Regimes in a Snowmelt-Dominated Basin

Amy L. Steimke ¹, Bangshuai Han ², Jodi S. Brandt ³ and Alejandro N. Flores ^{1,*}

¹ Department of Geosciences, Boise State University, Boise, Idaho

² Department of Geography, Ball State University, Muncie, Indiana

³ Human Environment Systems, Boise State University, Boise, Idaho

August 27, 2018

1 Abstract

2 Climate change directly affects the hydrologic cycle in mountainous watersheds, which has
3 consequences for downstream users. Improved water projections under diverse potential climate
4 futures are critical to improving water security and management in these watersheds. The hydro-
5 logic science researchers and water resource managers, however, often focus on different metrics
6 of flow regimes in changing climates. The research community tends to more closely focus on
7 biophysical state and flux variables of the hydrologic system. Managers, meanwhile, tend to fo-
8 cus on key administrative benchmarks that govern the operation of complex water storage and
9 distribution systems. Here, we examine potential hydrologic changes in a water supply basin in
10 the western United States in the context of both biophysical states and fluxes, as well as from
11 the perspective of how those changes map onto key variables that govern the administration of
12 water resources in the region. The study site consists of the Upper Boise River Basin, ID. This
13 snowmelt-dominated, mountainous watershed that supplies water to a semi-arid, agriculturally
14 intensive and rapidly urbanizing region. Using the Envision integrated modeling framework, we
15 created a hydrologic model and simulated hydrologic response to the year 2100 using six diverse
16 climate scenarios. Annual discharge increased from historical values by an average of 13% across

17 all climate scenarios with a range of increase of 6-24%, reflecting an increase in the precipitation
18 in the climate projections. Runoff timing was altered, with peak discharge occurring 4-33 days
19 earlier and center of timing of streamflow occurring 4-17 days earlier by midcentury. Examining
20 potential changes in the date junior water rights holders begin to be curtailed regionally (the Day
21 of Allocation), we found that the Day of Allocation occurs up to 14 days earlier by 2100 across all
22 climate scenarios, with one scenario suggesting this date could occur over a month earlier. These
23 results suggest that current methods and policies of water rights accounting and management
24 may need to be revised moving into the future.

25 **1 Introduction**

26 Climate change exerts a significant control on global hydrologic regimes by influencing the
27 timing, magnitude, phase, and seasonal variability in precipitation (Mote *et al.*, 2005; Regonda
28 *et al.*, 2005; Knowles *et al.*, 2006; Haddeland *et al.*, 2014). Changes in temperature further influence
29 how that precipitation moves through a watershed by affecting snowmelt timing, soil moisture,
30 and evapotranspiration rates (Barnett *et al.*, 2005; Li *et al.*, 2017). While there is general consensus
31 among scientists that the Earth is warming and will continue to do so, there remain significant
32 uncertainties regarding the impacts of global warming on the water cycle and how those changes
33 will be distributed regionally in the future (Huntington, 2006; Turrall *et al.*, 2011).

34 Significant changes in the water cycle can have serious consequences for water users and man-
35 agement across many sectors. It is estimated that more than two billion people currently live in
36 highly water-stressed regions (Oki, 2006), with this number projected to increase in the future
37 (Schewe *et al.*, 2014). Agriculture is vulnerable to changes in hydrologic regimes, especially in
38 regions that rely on surface water resources for irrigation and in rain-fed systems (Turrall *et al.*,
39 2011). Flooding could intensify, putting stress on current water management infrastructure as
40 well as lessening the effectiveness of hydropower generation as runoff arrives earlier (Markoff and
41 Cullen, 2008). Despite the seriousness of the potential impacts of hydrologic changes across sec-

42 tors, the effectiveness of current water management systems, practices, and policies under chang-
43 ing hydrologic regimes is not well understood.

44 Many previous modeling studies have investigated how water resources will respond to cli-
45 mate change in snowmelt-dominated systems (Adam *et al.*, 2009; Jin and Sridhar, 2011; Ficklin
46 *et al.*, 2013; Gergel *et al.*, 2017). However, results from such studies are not always presented in a
47 way that is usable to water managers and users. Here we provide an example of how hydrologic
48 modelers can generate results that may provide additional meaning for management decisions.
49 Managers of these systems tend to focus on the ways in which climate variability and change
50 will challenge existing water management protocols and practices. For example, in the American
51 West, there are often hierarchies of water rights users who may be affected differently by projected
52 changes in water availability (Vicuna *et al.*, 2007). Providing predictions more applicable to water
53 users requires more in-depth and location-specific knowledge of water management and distri-
54 bution but has the potential to provide more relevant information to a wider group of audiences.

55 Snowmelt-dominated systems, particularly those in the western U.S., are especially vulnerable
56 to climate change (Barnett *et al.*, 2005; Stewart, 2009; Li *et al.*, 2017). Significant reservoirs, in the
57 form of snow, develop at times (i.e., winter) and locations (i.e., high elevations) where that water
58 cannot be used to grow crops and produce hydroelectricity. This snowpack at high elevations
59 provides a natural reservoir that holds water in reserve and, ideally, slowly releases it into the
60 spring and summer, into downstream agricultural areas. A complex system of water rights and
61 management has been developed, and reservoir and canal systems engineered to store springtime
62 runoff, mitigate flooding, and direct it to other locations when there is a demand for irrigation.
63 This current system of water management infrastructure and protocols are set up to account for
64 the historical range of hydrologic variability; however, it may not be adequate to adapt to future
65 hydrologic regimes (Palmer *et al.*, 2008). With sufficient changes in the timing and magnitude of
66 water delivery, as is projected with climate change, current management practices may be inad-
67 equate to meet the dual needs of flood control and late-season irrigation demand (Barnett *et al.*,
68 2005). However, it is uncertain to what extent current management practices may be stressed un-

69 der future hydrologic regimes or when water management agencies can expect existing practices
70 and policies to begin coming into conflict with the reality of altered runoff regimes.

71 The overarching objective of this study is to better understand and quantify how climate
72 change will impact future water resources and water management in the context of metrics that
73 managers monitor and use to implement policy. We perform our study in the Upper Boise River
74 Basin, ID, an ideal location because it is a relatively undisturbed high mountain watershed that is
75 managed to provide water resources to an agriculturally-intensive and rapidly urbanizing region.
76 We explore this connected biophysical and social system by combining a surface water hydrologic
77 model with diverse climate projections to project potential changes in future regional hydrologic
78 regimes. Furthermore, we translate our model outputs into a metric that is directly applicable to
79 downstream water users and managers. Our specific research objectives are to:

- 80 1. Identify a range of climate projections and assess how they affect hydrologic parameters
81 such as center of timing of streamflow, volume of annual water delivery, and snowpack
82 levels through the end of the century; and
- 83 2. Identify how these changes in hydrologic regimes impact an associated metric that charac-
84 terizes water storage and is used to enforce water rights accounting policies.

85 What follows in this paper is: (1) a more detailed description of the study area, (2) an overview
86 of our methodological approach, (3) results of this study, and (4) discussion, implications, and
87 conclusions.

88 **2 Methods**

89 **2.1 Study Area**

90 The Upper Boise River Basin (UBRB) is located in southwest Idaho (Figure 1) and supplies
91 water for downstream users in the populated Boise metropolitan region. This watershed en-

92 compasses an area of 6,935 km² with elevation ranging from approximately 930 to 3,000 m. It
93 is bounded by the Sawtooth range in the east, the Payette River Basin to the north, and the Snake
94 River Plain to the southwest. We delineated the study area by combining three Hydrologic Unit
95 Code (HUC) 8 watersheds: the North and Middle Forks Boise (17050111), the South Fork Boise
96 (17050113), and Boise-Mores (17050112). Due to the large variation in topography throughout the
97 study area, regions shift from semi-arid grasslands and shrublands in the lowlands to coniferous
98 forests in the highlands. In the UBRB, the dominant land covers are forest (43.0%), shrubland
99 (34.6%) and grassland (20.9%), with sparse human development within the watershed. The cli-
100 mate in this region is a continental Mediterranean climate (Köppen *Dsb*) with cold winters, warm
101 summers, and the majority of precipitation falling in winter as snow. The overall average precip-
102 itation is ~800 mm, with averages ranging from ~400 mm at low elevations to over 1300 mm at
103 high elevations (Daly *et al.*, 2008).

104 The UBRB is the primary source of water for the downstream Treasure Valley region, which
105 contains the state's three largest cities (Boise, Nampa, and Meridian) and roughly 40% of the
106 state's total population. The Treasure Valley is an agriculturally intensive region and contains
107 approximately 1300 km² of farmlands, many of which rely on irrigation water from the UBRB.
108 Like many other snowmelt-dominated watersheds in the West, the UBRB is heavily managed via
109 three large storage reservoirs to fulfill the needs of flood control and downstream uses, especially
110 for direct consumption in the Treasure Valley. Similar to other western states, water rights in this
111 region follow the Prior Appropriation Doctrine, also known as "first in time – first in right." This
112 doctrine states that the earliest beneficial users (i.e., senior water rights) retain their full water
113 right, and those that came later (i.e., junior water rights) may retain their water rights as long
114 as they do not infringe on those that came beforehand. As such, many junior water rights are
115 curtailed during low water years, as total surface water rights in the Treasure Valley surpass 14,000
116 ft³/s, far exceeding the natural flow of the Boise River.

117 Previous studies indicate that the UBRB has already begun to respond hydrologically to cli-
118 mate change, noting an increase in summer streamflow temperatures (Isaak *et al.*, 2010), earlier

119 timing of streamflow (Clark, 2010), lengthened growing season (Kunkel, 2004), and declining ex-
120 treme low flow discharges (Kormos *et al.*, 2016). Additionally, there have been previous modeling
121 studies that have used this basin to anticipate changes in hydrology under climate change (Still-
122 water, 2008; Jin and Sridhar, 2011). However, both of the aforementioned studies used an older
123 generation of global climate models as their climate input and calibrated their models to stream-
124 flow alone. This study extends those previous works by making use of climate projections from
125 the 5th Coupled Model Intercomparison Project (CMIP5, Taylor *et al.*, 2012), calibrating the hydro-
126 logic model to multiple hydrologic metrics, and producing results that may provide additional
127 meaning to water users.

128 **2.2 Modeling Framework**

129 Here we employ the Envision framework, a multiagent-based, spatially explicit modeling
130 framework, to examine how regional hydrology may change with climate. Envision was cre-
131 ated to examine relationships between human and natural environmental systems by integrating
132 scenarios, data, and component models to assess regional landscape change (Bolte *et al.*, 2007). To
133 this end, the modeling framework and software infrastructure of Envision support the integra-
134 tion of a variety of social and biophysical models in a spatiotemporally dynamic way. It is freely
135 available and users can extend and enhance model capabilities by adding additional models as
136 plugins. It has been extensively used recently in a wide variety of studies, from understanding
137 urbanization impacts on streamflow (Wu *et al.*, 2015) to projecting climate change impacts of land
138 cover and land use (Turner *et al.*, 2015), and even to understand when fire occurrence and size is
139 'surprising' (Hulse *et al.*, 2016). Additionally, it has been used to integrate water rights to spatially
140 allocate irrigation in the agriculturally intensive region below the UBRB (Han *et al.*, 2017).

141 In this study, we use Envision version 6.197 and utilize the Flow extension to model future
142 hydrology under various climate scenarios. In the following sections, we provide an overview of
143 the modeling structure and the inputs needed for the various components.

144 2.2.1 Spatial Coverage in Envision

145 In Envision, the most refined spatial elements where model algorithms are applied are referred
146 to as Integrated Decision Units (IDUs). The size and geometry of these polygons are dependent
147 on the type of modeling being performed and the geospatial datasets required as input to those
148 models. As such, there is no universally accepted method for creating IDU coverage. In this study,
149 we used three datasets to form the IDU geometry: surface management agency, land cover, and
150 HUC 12 stream catchments (Table 1). As such, the IDU coverage will preserve boundaries be-
151 tween HUC 12 catchments, cognizant land management agencies, as well as boundaries between
152 vegetation classes.

153 The datasets were processed in ArcMap 10.1. To shorten Envision's computation time, we
154 coarsened the land cover dataset from 30 to 100 m in increments of 10 m. We used a nearest neigh-
155 bor algorithm to resample land cover types to more accurately capture the original distribution
156 of coverage in the land cover dataset. The other two datasets were polygon geospatial datasets
157 that required very little processing besides renaming attributes to be consistent with the Envision
158 framework requirements.

159 We created our IDU coverage by intersecting the three aforementioned datasets, creating 31,625
160 polygons. We extracted the average elevation for each IDU and also assigned an elevation class
161 from 1-4, corresponding to 0-1500, 1500-2000, 2000-2500, and >2500 meters to allow binning and
162 analysis of results by elevation band. Additionally, to aid in analysis and querying we created a
163 three-tiered hierarchy of land cover classification ranging from general (e.g. Natural Vegetation)
164 to more specific (e.g. Evergreen Forest), which was formed by grouping NLCD classifications that
165 are similar (Figure 2).

166 The hydrologic model in Envision applies algorithms to Hydrologic Response Units (HRUs, Jin
167 and Sridhar, 2011; Turner *et al.*, 2016), which are an aggregation of IDUs that would theoretically
168 behave hydrologically similar. To create the HRU coverage, we grouped polygons that had the
169 same intermediate land cover (Figure 2), identical elevation class, and were located in the same

170 HUC-12 catchment. This resulted in 9,465 HRUs.

171 2.2.2 Hydrologic System Model

172 An extension in Envision called Flow provides flexibility in modeling hydrology and the use of
173 different model representations of hydrologic processes. In this study, we used a modified version
174 of the HBV (Hydrologiska Byråns Vattenbalansavdelning) rainfall-runoff model (Bergström, 1976)
175 for surface hydrology. HBV is a commonly used conceptual model (Seibert, 2000; Woodsmith *et al.*,
176 2007; Abebe *et al.*, 2010; Bergström and Lindström, 2015) but has been modified by Envision's
177 developers to be spatially distributed. Each HRU is conceptualized as a linked reservoir with five
178 layers of storage: snowpack, lakes, soil, upper groundwater, and lower groundwater (Figure 3).
179 Runoff from each HRU is routed to streams using HUC12 flowlines from NHDplus V2 (Table 1).
180 The water balance in Flow is described by the following equation:

$$P - ET - Q = \frac{d}{dt} [SP + SM + UZ + LZ + lakes] \quad (1)$$

181 where P is precipitation [mm/d], ET is evapotranspiration [mm/d], Q is runoff [mm/d],
182 SP is snow storage [mm], SM is soil moisture storage [mm], UZ is upper groundwater storage
183 [mm], LZ is lower groundwater storage [mm], and $lakes$ refers to lake storage [mm]. A more
184 thorough description of the HBV model can be found in other papers (Seibert, 1999; Bergström
185 and Lindström, 2015) and a more detailed description of Flow can be found on Envision's website
186 (<http://envision.bioe.orst.edu/>).

187 Evapotranspiration (ET) is calculated via a modified Penman-Monteith approach described in
188 the Food and Agriculture Organization's Irrigation and Drainage paper 56 (FAO56) where a crop
189 coefficient is applied to the ET of a reference plant (Allen *et al.*, 1998) and was later developed
190 specifically for Idaho (Allen and Robison, 2007) using the following equation:

$$ET = ET_r \cdot K_c \quad (2)$$

191 where ET = evapotranspiration, ET_r = reference evapotranspiration (alfalfa, for Idaho), and K_c
192 = crop coefficient.

193 We used this equation and applied crop coefficient curves that either matched our land cover
194 type directly or estimated crop coefficient curves based upon similarities of crops to land cover
195 types (Table 2). Crop coefficients were obtained from AgriMet and (Allen and Robison, 2007),
196 with a few modified land cover coefficients from (Inouye, 2014).

197 **2.3 Climate Inputs**

198 We used statistically downscaled climate data using the MACA (Multivariate Adaptive Con-
199 structed Analogs) method version 1.0 for both historic and future simulations (Abatzoglou and
200 Brown, 2011). This data has a spatial resolution of 4 km across the continental U.S. and is avail-
201 able daily for 1950-2100. Downscaled data is available for 20 Global Climate Models (GCMs) from
202 CMIP5 for both Representative Concentration Pathway (RCP) 4.5 and 8.5 scenarios. RCPs are a
203 consistent set of projections that are named according to their additional radiating forcing level at
204 2100, such that RCP 4.5 equates to $+4.5 \text{ W/m}^2$ radiative forcing relative to pre-industrial values
205 by the end of the century (van Vuuren *et al.*, 2011).

206 For future simulations, we selected GCMs based upon two criteria. First, we halved our GCM
207 selection to models that performed relatively well when ran over the historical period in the Pacific
208 Northwest region (Rupp *et al.*, 2013), meaning they produced less relative error when compared
209 across several metrics. Secondly, we selected GCMs that captured the range of variability between
210 models as it related to changes in precipitation and temperature (Figure 4). We selected three
211 climate models: CanESM2 (hotter, wetter), CNRM-CM5 (warmer, slightly wetter), and GFDL-
212 ESM2M (less warm, drier), and ran each one for RCP 4.5 and 8.5 scenarios, which resulted in
213 six total future climate scenarios (Figure 5). Table 3 provides a naming convention for these six
214 future climate scenarios to ease in discussing results and implications. For historical simulations
215 from 1980-2014, we used a historical climate dataset, METDATA (Abatzoglou, 2011), which was
216 developed using data from the North American Land Data Assimilation System Phase 2 (NLDAS-

217 2, Mitchell, 2004) and from the Parameter-elevation Regressions on Independent Slopes Model
218 (PRISM, Daly *et al.*, 2008).

219 The downscaled variables Envision requires for Flow are daily maximum, minimum, and aver-
220 age temperature, precipitation amount, specific humidity, daily downward shortwave radiation,
221 and wind speed. To format the variables for Envision, the following procedure was followed:
222 (1) subset data to the specified region, (2) convert units and rename variables where needed, (3)
223 compute average temperature as the average between minimum and maximum temperature, (4)
224 calculate overall wind speed from the eastward and northward components provided by MACA,
225 and (5) subset into annual files. Scripts created for pre-processing MACA climate data are avail-
226 able online at https://github.com/asteimke/MACA_EnvisionClimate.

227 **2.4 Calibration and Validation**

228 HBV is a semi-conceptual model, and as such, parameters required as input to the model are
229 obtained through calibration because most parameters cannot be physically measured (Bergström
230 and Lindström, 2015). Numerous combinations of parameter values can yield equally good re-
231 sults (i.e. the equifinality issue, Beven, 2006; Gupta *et al.*, 2005), which makes it difficult to select
232 the best parameter set. To combat this issue, some studies (Madsen, 2003; Inouye, 2014) build
233 an objective function to find an adequate parameter set based on the type of information they
234 want to yield from the model (e.g. streamflow volume, timing, snowpack, etc.). Typically, the
235 calibration-validation procedure takes the form of a data-denial experiment. The model is run
236 over a calibration period to select best parameter sets and then re-run over a validation period to
237 ensure that the selected parameter set performs well during this period for which data was not
238 used to calibrate the model.

239 Fourteen parameters are included within the HBV model and govern rates of exchange be-
240 tween reservoirs. We held five of them constant, while the remaining nine were calibrated. *CFR*
241 and *CWH* are insensitive parameters and were held constant as is often done in HBV applications
242 (Seibert, 1997). While many of the parameters are conceptual and cannot be measured, three of

243 them are based on physical properties, so we fixed those parameters to better represent the reality
 244 of our study area. We used the Global Gridded Surfaces of Selected Soil Characteristics (IGBP-
 245 DIS) dataset (Hope and Peck, 1994) and took the average of values for the study area. We used the
 246 following datasets from IGBP-DIS: soil field capacity, soil profile available water capacity, and soil
 247 wilting point for the parameters FC , LP , and WP , respectively (Table 4). In each model run, we
 248 randomly selected the remaining nine parameters from a uniform distribution between ranges of
 249 possible values (Table 4) defined based on previous studies (Inouye, 2014; Han *et al.*, 2017).

250 We ran the model for 1000 simulations at a daily time step over the years 1988-2000 (12 years +
 251 1 spin-up year). We selected this time interval for calibration because it encompasses a reasonably
 252 long time period and includes both wet and dry years. We compared model output to historical
 253 stream discharge records from three long-term USGS gaging stations and snowpack observations
 254 from nine SNOTEL (SNOW TELEmetry) stations, omitting all leap days from these datasets (Table
 255 5). For each run, we calculated the Nash-Sutcliffe Efficiency (NSE , Nash and Sutcliffe, 1970),
 256 $\log NSE$, and a volume error (VE) using the following equations:

$$NSE = 1 - \frac{\sum_{t=1}^T (Q_{obs}^t - Q_{sim}^t)^2}{\sum_{t=1}^T (Q_{obs}^t - \overline{Q_{obs}})^2} \quad (3)$$

$$\log NSE = 1 - \frac{\sum_{t=1}^T (\ln Q_{obs}^t - \ln Q_{sim}^t)^2}{\sum_{t=1}^T (\ln Q_{obs}^t - \ln \overline{Q_{obs}})^2} \quad (4)$$

$$VE = \frac{\sum_{t=1}^t (Q_{obs}^t - Q_{sim}^t)}{\sum_{t=1}^t (Q_{obs}^t)} \quad (5)$$

257 where Q_{obs} is the observed value and Q_{sim} is the simulated value at each daily time step.

258 NSE coefficients range from $-\infty$ to 1, with 1 indicating a perfect fit of the model to the ob-
 259 served data, and a value of $NSE > 0$ indicating the model is a better predictor than the historically
 260 observed mean. Typically, a model is deemed satisfactory if the NSE is larger than 0.5 (Moriasi
 261 *et al.*, 2007). The logarithmic form of the NSE also ranges from $-\infty$ to 1, but is more sensitive to

262 low flow and still reacts to peak flows (Krause *et al.*, 2005). The volume error provides insight into
263 whether the model overestimates ($VE < 0$) or underestimates ($VE > 0$) total volume, with a value
264 closest to 0 being ideal.

265 We created an objective function to select the best-performing parameter set and was devel-
266 oped based on work by (Inouye, 2014):

$$Obj = \frac{1}{3} (NSE_G) + \frac{1}{3} (\log NSE_G) + \frac{1}{3} (NSE_S) - 0.2 \cdot |VE_G| \quad (6)$$

267 where NSE_G is the Nash-Sutcliffe Coefficient of discharge weighted by an areal average of the
268 gauges, VE_G is the volume error for the gauges weighted by an areal average, and NSE_S is the
269 averaged Nash-Sutcliffe Coefficient for SWE (snow water equivalent) for all SNOTEL sites.

270 The objective function ideally is as close to 1 as possible, as we wish to maximize NSE and
271 minimize volume bias. The top 1% best performing parameter sets were run over the eight-year
272 validation period (2001-2008) and the set that performed on average the best in both calibration
273 and validation years was chosen for our model. Results of the calibration/validation exercises are
274 reported in the Results section of this manuscript.

275 2.5 Evaluating Climate Change Impacts

276 To assess the potential impact of climate change on hydrologic regimes, we examined three
277 broad metrics: streamflow, snowpack, and water management. A more detailed description of
278 methods for these metrics is described here.

279 2.5.1 Streamflow

280 While Envision has the capability to examine discharge values anywhere along its stream net-
281 work, we focused here on the aggregation of streamflows for the basin. In all cases, unless men-
282 tioned otherwise, streamflow results are for the unregulated discharge on the Boise River occur-
283 ring at the location of Lucky Peak Dam's outlet, i.e. the pourpoint of the watershed (Figure 1).

284 This modeled streamflow, as well as daily values for the three major tributaries, can be obtained
285 online (Steimke *et al.*, 2017).

286 To assess climate change impacts on streamflow, we looked at changes in the amount and
287 timing of discharge. An additional metric we used was the center of timing (CT) of streamflow,
288 which is the date when half of the annual volume of water during the water year has arrived
289 at a specified location. We calculated the CT for historical data and future simulations with the
290 following equation (Stewart *et al.*, 2005):

$$CT = \frac{\sum (t_i Q_i)}{\sum Q_i} \quad (7)$$

291 where t_i is the time in days from the start of the water year (October 1) and Q_i is the discharge
292 for that date.

293 2.5.2 Snowpack

294 To assess climate impacts on the basin's snowpack, we looked at averaged values over three
295 elevation zones: low (1500-2000 m), medium (2000-2500 m), and high (2500+ m) zones. These
296 zones cover 43.4%, 25.8%, and 6.9% of the area of interest, respectively. We do not show results
297 for elevations less than 1500 m as the lowest SNOTEL station to aid in calibration is the Prairie site
298 at 1463 m. Within these three zones, we examine the dates and magnitudes of when SWE is at its
299 maximum, as well the April 1 SWE amount. Water managers have historically used the amount
300 of SWE on this date as an indicator for water availability in the upcoming year, as it has correlated
301 well with maximum SWE at many SNOTEL sites in the West historically (Bohr and Aguado, 2001).

302 2.5.3 Water Management

303 Since 1986, water managers annually declare a Day of Allocation (DOA) in the Lower Boise
304 River Basin for the purpose of water rights accounting during the irrigation season (April – Oc-
305 tober). This day is declared on or after the date of maximum reservoir fill and once natural flow

306 is less than irrigation demand (Memo from IDWR Technical Hydrologist Liz Cresto to IDWR Di-
307 rector Gary Spackman, November 4, 2014, Subject: Accounting for the distribution of water to
308 the federal on-stream reservoirs in Water District 63). The DOA occurs after peak runoff and has
309 been shown historically to typically occur once the natural flow of the Boise River at Lucky Peak
310 reaches below 4000 ft³/s (Garst, 2017), or 113.3 m³/s (Figure 6), which is roughly equivalent to
311 the diversion demand of the river. It is beneficial for farmers if the DOA occurs later in the season
312 because after the DOA is declared water rights begin to be curtailed, starting with the junior-
313 most water rights holders. While the term DOA is unique to three major river basins in Idaho
314 (i.e. Boise, Payette, and Upper Snake river basins), many western states have similar methods for
315 appropriating water as the irrigation season begins.

316 To predict how the DOA may change in our modeled scenarios, we assume that diversion
317 rights will continue to be approximately 113.3 m³/s. We model our DOA date by finding the last
318 day during peak runoff during the irrigation season that flow is greater than 113.3 m³/s and select
319 the day after. We then manually observe the hydrographs and the DOA selected to ensure we are
320 capturing a date on the downfalling limb of peak runoff and not a later season event. If a later
321 season event was modeled, then we manually select the date on which modeled flow falls below
322 113.3 m³/s during the recession limb of spring runoff. We ran the model during the historical
323 period to investigate how well the model reproduces historical DOA using this definition, which
324 provides confidence in our interpretation of DOA changes in modeled future scenarios.

325 **3 Results**

326 **3.1 Calibration and Validation**

327 We calibrated and validated the model using historical records from three USGS gauges and
328 nine SNOTEL sites. The parameter set that performed best had an objective function score of 0.63
329 and 0.62 for calibration and validation periods, respectively (Table 6). We averaged the NSE for

330 each gauge by its respective drainage area, which resulted in a *NSE* of 0.71 and 0.70 for calibration
331 and validation, respectively. However, it should be noted that Mores Creek on its own achieved
332 a lesser *NSE* of 0.58, which is potentially due to this smaller watershed exhibiting some major
333 differences from the other two (notably lower elevation, less precipitation, and less steepness).

334 Among all gauges, we see relatively good agreement between the model simulations and ob-
335 served flow for the historic period (Figure 7), although the model frequently under predicts the
336 magnitude of peak flows at all gauge sites and over predicts baseflow at Mores Creek. While the
337 unregulated flow for the Boise River at Lucky Peak (Table 5) was not used to calibrate the model,
338 we used this as an additional verification dataset to ensure accuracy of the model. With the cho-
339 sen parameter set, we achieved a *NSE* at this site of 0.74 and *VE* of -0.01 averaged over the entire
340 calibration and validation period, providing additional confidence in our model.

341 **3.2 Streamflow**

342 **3.2.1 Annual Discharge**

343 In all future climate scenarios, we see an increase in the median annual discharge from the
344 Boise River (Figure 8). By midcentury (2040-2069), all climate scenarios showed an increase in an-
345 nual discharge over historical (1950-2009) averages, with an average increase of 13% and ranges
346 of increase from 6-24%. RCP 8.5 climate scenarios showed a greater rate of increase over RCP
347 4.5 scenarios. Because our hydrologic model did not perform well historically in accurately cap-
348 turing the magnitude of peak discharges, we do not have adequate confidence to predict future
349 magnitudes in peak or low flows.

350 **3.2.2 Timing of Discharge**

351 While we see some changes in the volume of annual discharge, streamflow is also projected to
352 arrive at significantly different times than in the historical past. However, these arrival times vary
353 greatly between different climate models.

354 In most future climate scenarios, the date of peak discharge occurs earlier in the season, with
355 an increase in early winter flooding events (Figure 9). In extreme climate cases (i.e. C-85), the
356 average peak discharge occurs approximately 45 days earlier in the period 2040-2060 relative to
357 1980-2009. In a conservative climate model (i.e. A-45), peak discharge may only be on average
358 about 5 days earlier by midcentury.

359 To get an understanding of the shift in seasonality and variance between climate scenarios,
360 we can look at the multi-decadal averaged hydrographs between two endmember climate models
361 predicting the least and most amount of change from historical averages (Figure 10). With the
362 coolest climate scenario (A-45), there is little discernible deviation from the historical average hy-
363 drograph. However, if we look at the warmest climate scenario (C-85), we see obvious differences
364 in the average hydrograph, where by 2050-2070 the average peak of the hydrograph is over a
365 month and a half earlier. Overall, this warmest scenario shows a shift in seasonality through time,
366 where we see flows occurring earlier in the season with an additional increase in early-season,
367 mid-winter discharge events.

368 **3.2.3 Center of Timing**

369 The historical average (1980-2009) center of timing (CT) of streamflow for the UBRB is April 22.
370 In our simulations, we see this date shift earlier in most of our climate scenarios (Figure 11). Three
371 scenarios (C-45, B-45, and A-85) behave similarly and begin deviating from the historical range
372 of variability between 2040 and 2050, showing a CT date that is 13-17 days earlier on average
373 between 2070 and 2099. Both C-85 and B-85 begin to deviate from historical averages around 2030
374 and exhibit an average a CT date 27-30 days earlier than the historical average during the 2070-
375 2099 period. A-45 remains relatively similar to historical ranges through the century, although its
376 CT date shifts a few days earlier, resulting in fewer occurrences of exceeding the historical 75th
377 percentile of CT date.

378 3.3 Snowpack

379 3.3.1 April 1 SWE

380 Our results (Figure 12) show a substantial decrease in April 1 SWE in five of the climate sce-
381 narios, with lower elevations essentially experiencing no April 1 SWE by midcentury. Higher ele-
382 vations remain less affected across all RCP 4.5 scenarios but begin substantially decreasing around
383 2050 in B-85 and C-85 where they experience virtually no April 1 SWE from 2080-2100. Under the
384 A-45 scenario, April 1 SWE experiences variability, but has no discernible downward trend.

385 3.3.2 Dates and amounts of maximum SWE

386 The previous section suggests that April 1 SWE will, at some point in the future, cease to be a
387 good indicator of maximum SWE. In terms of evaluating potential climate change impacts on SWE
388 in the context of water supply, therefore, it is necessary to examine additional metrics. Specifically,
389 we see the date of maximum SWE happening earlier across most scenarios (Figure 13). Both C-85
390 and B-85 show maximum SWE occurring more than two months earlier on average by the end
391 of the century. Three scenarios, A-85, C-45, and B-45 behave similarly with maximum SWE date
392 happening between 38 and 42 days earlier than historically observed averages. A-45 produces
393 little change in timing by the end of the century (7 days earlier on average).

394 The magnitudes of maximum SWE may change as well (Figure 14). Within mid-elevation
395 zones (2000-2500 m), we see a drastic decrease in the occurrence of annual amounts above the
396 historical 75th percentile in five of our climate scenarios. Furthermore, from 2050 onward, we see
397 that 80% (C-85) and 84% (B-85) of the time the maximum SWE is falling below the historical 25th
398 percentile. As with many of the metrics previously mentioned, A-45 shows very little change from
399 historical trends.

400 3.4 Water Management

401 3.4.1 Day of Allocation

402 The developed model reasonably reproduces the DOA in the historical period ($R^2=0.90$), al-
403 though it over-predicted the date on average 4.8 days later (Figure 6). Thus, the defined metric for
404 the DOA provides a reasonably robust vehicle to analyze how the DOA may shift under different
405 climate scenarios. Our results show the DOA occurring much earlier under four of our scenarios
406 (Figure 15), ranging from 11 to 33 days earlier on average by the end of the century. Scenarios A-45
407 and B-45 resulted in little to no change in the trend of DOA. While the DOA remains variable on
408 an interannual basis, we do not see significant changes in variability of DOA through time (Table
409 7).

410 4 Discussion

411 4.1 Trends in Future Hydrologic Regimes

412 We calibrated our model using metrics that included historic snowpack levels, daily stream-
413 flow, logarithmic transformation of streamflow, and streamflow volume. Choosing multiple met-
414 rics to select the best parameter set provides some additional confidence that the model is sim-
415 ulating key attributes of historical hydrologic regimes and, therefore, strengthens confidence in
416 the robustness of our interpretations of future climate change impacts on hydrologic regimes pre-
417 dicted by the model.

418 We have shown that a variety of hydrologic regime characteristics within the UBRB could ex-
419 hibit significant changes, depending on which climate model and RCP scenario is used. However,
420 certain trends are consistent across several considered climate scenarios and are consistent with
421 other projections (Adam *et al.*, 2009; Inouye, 2014; Gergel *et al.*, 2017). Our results suggest an in-
422 crease in annual water discharge, but with significantly altered timing, with flows arriving much

423 earlier than historically. Our modeled results also show a decrease in the total amount of snow-
424 pack, an earlier melting date, and earlier dates of peak snowpack. In order to reconcile how annual
425 discharge can increase while the snowpack is consistently smaller in volume and more ephemeral
426 in time, we examined the seasonality of the precipitation input to the model. This allows us to bet-
427 ter understand whether observed changes in discharge volume are primarily related to changes
428 in the seasonality of input precipitation, changes in the seasonal dynamics of snowpacks, or some
429 combination of both. Typically, however, the precipitation exhibits increases across all seasons
430 rather than large shifts between seasons in precipitation. Accordingly, this may indicate that the
431 basin could begin transitioning from being snowmelt-dominated to a regime that is mixed rain-
432 and snow-dominated watershed moving forward.

433 **4.2 Management Implications**

434 Our modeled scenarios support previous studies (Pederson *et al.*, 2011; Klos *et al.*, 2014) that
435 April 1 SWE is not likely to remain a reliable metric for estimating maximum SWE (and therefore
436 snow water storage) in the future for water resource prediction and management. This work
437 suggests declines in the amount of SWE on April 1 and a maximum SWE date over a month earlier
438 than historically observed in five of the six considered scenarios. Rather than choosing a static
439 date to estimate peak SWE across a vast region, managers may need to more closely monitor the
440 relationship between hydrologic regimes and the timing of peak SWE in their regions, potentially
441 necessitating increased investment in monitoring and modeling of snow conditions.

442 There is little evidence to conclude that we will experience future water shortages from the
443 UBRB in an absolute sense, as most models suggest at least a small increase in annual discharge.
444 However, we will likely experience hydrologic shifts that are outside of our current range of vari-
445 ability. All climate scenarios show peak discharge occurring earlier in the year. This is problematic
446 for reservoir managers who primarily manage dams to provide storage for flood mitigation. Man-
447 agers might have to release more 'usable' water from reservoirs in preparation for these events,
448 which potentially could equate to shortages later in the irrigation season. Such outcomes could be

449 viewed as an "operational deficit" that arises because of a mismatch between the release of water
450 from storage for flood mitigation and the timing of water allocation as codified in water rights
451 laws.

452 At the same time, in this region agricultural land is increasingly transitioning to urban areas
453 (Dahal *et al.*, 2017), which could indicate that future water demand may be substantially differ-
454 ent from the past. With warmer climates, farmers might plant earlier in the season, which would
455 change the timing of water demand. Recent modeling efforts have shown that current water rights
456 are not always able to support irrigation demand (Han *et al.*, 2017). Agricultural water use effi-
457 ciency, however, is likely to increase with technological advances like genetically modified crops,
458 which could change spatiotemporal patterns of water demand. A more comprehensive examina-
459 tion of how, when, and where water is being used downstream and how that may change in the
460 future will help managers understand to what extent regional water infrastructure is vulnerable
461 and the potential policies that might help to mitigate effects.

462 Our results show that under most climate scenarios, the Day of Allocation occurs much earlier
463 than it has historically, with two models showing the date moving by over a month earlier. If this
464 projection becomes reality, then there is an earnest need for exploring potential conflicts between
465 water users in the future as curtailments may come increasingly early and impact more water
466 rights holders than in previous decades. It may be necessary, for instance, to incentivize farmers
467 to transition to more efficient irrigation practices (e.g. switching from flood to drip irrigation)
468 and to diversify with crops that require less water, or expand other solutions like water bank-
469 ing and water markets. If junior water rights holders are curtailed over a month earlier without
470 any mitigation practices set in place, it may result in substantial repercussions to Idaho's agricul-
471 tural sector. These effects are compounded if other mountain water supply basins exhibit similar
472 changes to hydrologic regimes.

473 **4.3 Study Limitations**

474 It is worth noting that this study did not simulate reservoir operations. There are three dams
475 present in the study area that are located close to the outlet of the basin. For purposes of simplicity,
476 the present work focuses on evaluating the ramifications of climate change on natural flows in the
477 UBRB and capturing reservoir operations is outside the scope of this study. A significant challenge
478 in future work will arise from the need to develop plausible scenarios by which water managers
479 from federal agencies, irrigation districts, environmental groups, and utility companies can create
480 strategies to adapt to potential changes in hydrologic regimes similar to those simulated here.
481 Given the complexities in both biophysical and social responses to climate change, such studies
482 will likely need to be region- and context-specific.

483 An additional source of uncertainty in this study lies in the land cover data used in the hy-
484 drologic model, which was treated as static. Specifically, the land cover dataset used represents
485 a snapshot estimated based on Landsat reflectances from 2011. Vegetation along ecotones is sen-
486 sitive to changes in climate, and there are likely to be additional large-scale vegetation and land
487 cover changes that occur after wildfire events or through land management actions. Future mod-
488 eling studies should incorporate plausible shifts in vegetation to understand the sensitivity of
489 changes in hydrologic regimes to associated changes in land cover as well as climate change. This
490 might be best accomplished using a physically-based model, rather than the conceptual model
491 used in this study, to be able to better capture complex interactions between climate, hydrology,
492 vegetation dynamics, and changing land cover.

493 **4.4 Conclusions**

494 In this study, we used an integrated modeling framework, Envision, to simulate future hy-
495 drology in a mountainous watershed that supports an urban and agriculturally intensive region
496 below it. We calibrated the hydrologic model to metrics of both streamflow and snowpack, and it
497 performed well under historical conditions. We ran the model to the year 2100 under six climate

498 scenarios (three GCMs and two RCP scenarios) to analyze future possible hydrologic regimes.

499 Our results suggest that overall annual streamflow will increase, and five of six scenarios sug-
500 gest hydrologic regimes that will deliver runoff substantially earlier than historically observed.
501 This could lead to operational water shortages later in the season as water managers balance re-
502 lease of water from storage in reservoirs to mitigate flooding hazards with retention of water for
503 supplying irrigation in the warm, dry summers. Without changes in existing policies, these hydro-
504 logic regimes could have repercussions to late-season irrigation demand, hydropower operations,
505 recreational flows, and municipal water supply.

506 Mountainous, snowmelt-dominated watersheds have already begun responding to climate
507 change, which will almost certainly continue in the future. The degree to which the runoff re-
508 sponse of these watersheds changes in association with climate change is uncertain, and will
509 depend heavily on the nature of the change in the climatic forcing variables. Increasingly so-
510 phisticated comparisons with climate model predictions and observations, as well as regionally
511 focused and contextual modeling of coupled hydrologic and social systems, will improve our abil-
512 ity to constrain how hydrologic regimes will change in the future. This may increase the efficacy
513 of efforts to respond to changes and potential conflicts between potentially competing demands
514 for water.

515 **Acknowledgments**

516 This study was made possible with funding support from NSF CAREER award EAR-1352631,
517 and NSF Established Program to Stimulate Competitive Research award IIA-1301792.

518 **References**

519 Mote, P.W.; Hamlet, A.F.; Clark, M.P.; Lettenmaier, D.P. Declining Mountain Snowpack in Western
520 North America. *Bulletin of the American Meteorological Society* **2005**, *86*, 39–50.

521 Regonda, S.K.; Rajagopalan, B.; Clark, M.; Pitlick, J. Seasonal Cycle Shifts in Hydroclimatology
522 over the Western United States. *Journal of Climate* **2005**, *18*, 372–384.

523 Knowles, N.; Dettinger, M.D.; Cayan, D.R. Trends in Snowfall versus Rainfall in the Western
524 United States. *Journal of Climate* **2006**, *19*, 4545–4559.

525 Haddeland, I.; Heinke, J.; Biemans, H.; Eisner, S.; Flörke, M.; Hanasaki, N.; Konzmann, M.; Lud-
526 wig, F.; Masaki, Y.; Schewe, J.; Stacke, T.; Tessler, Z.D.; Wada, Y.; Wisser, D. Global water re-
527 sources affected by human interventions and climate change. *Proceedings of the National Academy*
528 *of Sciences* **2014**, *111*, 3251–3256.

529 Barnett, T.P.; Adam, J.C.; Lettenmaier, D.P. Potential impacts of a warming climate on water
530 availability in snow-dominated regions. *Nature* **2005**, *438*, 303–309.

531 Li, D.; Wrzesien, M.L.; Durand, M.; Adam, J.; Lettenmaier, D.P. How much runoff originates as
532 snow in the western United States, and how will that change in the future? *Geophysical Research*
533 *Letters* **2017**, *44*, 6163–6172.

534 Huntington, T.G. Evidence for intensification of the global water cycle: Review and synthesis.
535 *Journal of Hydrology* **2006**, *319*, 83–95.

536 Turrall, H.; Burke, J.J.; Faurès, J.M. *Climate change, water and food security*; Food and Agriculture
537 Organization of the United Nations Rome, Italy, 2011.

538 Oki, T. Global Hydrological Cycles and World Water Resources. *Science* **2006**, *313*, 1068–1072.

539 Schewe, J.; Heinke, J.; Gerten, D.; Haddeland, I.; Arnell, N.W.; Clark, D.B.; Dankers, R.; Eisner, S.;
540 Fekete, B.M.; Colón-González, F.J.; Gosling, S.N.; Kim, H.; Liu, X.; Masaki, Y.; Portmann, F.T.;
541 Satoh, Y.; Stacke, T.; Tang, Q.; Wada, Y.; Wisser, D.; Albrecht, T.; Frieler, K.; Piontek, F.; Warsza-
542 wski, L.; Kabat, P. Multimodel assessment of water scarcity under climate change. *Proceedings*
543 *of the National Academy of Sciences* **2014**, *111*, 3245–3250.

544 Markoff, M.S.; Cullen, A.C. Impact of climate change on Pacific Northwest hydropower. *Climatic*
545 *Change* **2008**, *87*, 451–469.

546 Adam, J.C.; Hamlet, A.F.; Lettenmaier, D.P. Implications of global climate change for snowmelt
547 hydrology in the twenty-first century. *Hydrological Processes* **2009**, *23*, 962–972.

548 Jin, X.; Sridhar, V. Impacts of Climate Change on Hydrology and Water Resources in the Boise
549 and Spokane River Basins¹. *JAWRA Journal of the American Water Resources Association* **2011**,
550 *48*, 197–220.

551 Ficklin, D.L.; Stewart, I.T.; Maurer, E.P. Climate Change Impacts on Streamflow and Subbasin-
552 Scale Hydrology in the Upper Colorado River Basin. *PLoS ONE* **2013**, *8*, e71297.

553 Gergel, D.R.; Nijssen, B.; Abatzoglou, J.T.; Lettenmaier, D.P.; Stumbaugh, M.R. Effects of climate
554 change on snowpack and fire potential in the western USA. *Climatic Change* **2017**, *141*, 287–299.

555 Vicuna, S.; Maurer, E.P.; Joyce, B.; Dracup, J.A.; Purkey, D. The Sensitivity of California Water Re-
556 sources to Climate Change Scenarios. *JAWRA Journal of the American Water Resources Association*
557 **2007**, *43*, 482–498.

558 Stewart, I.T. Changes in snowpack and snowmelt runoff for key mountain regions. *Hydrological*
559 *Processes* **2009**, *23*, 78–94.

560 Palmer, M.A.; Reidy Liermann, C.A.; Nilsson, C.; Flörke, M.; Alcamo, J.; Lake, P.S.; Bond, N.
561 Climate change and the world's river basins: anticipating management options. *Frontiers in*
562 *Ecology and the Environment* **2008**, *6*, 81–89.

563 Daly, C.; Halbleib, M.; Smith, J.I.; Gibson, W.P.; Doggett, M.K.; Taylor, G.H.; Curtis, J.; Pasteris, P.P.
564 Physiographically sensitive mapping of climatological temperature and precipitation across the
565 conterminous United States. *International Journal of Climatology* **2008**, *28*, 2031–2064.

566 Isaak, D.J.; Luce, C.H.; Rieman, B.E.; Nagel, D.E.; Peterson, E.E.; Horan, D.L.; Parkes, S.; Chan-

567 dler, G.L. Effects of climate change and wildfire on stream temperatures and salmonid thermal
568 habitat in a mountain river network. *Ecological Applications* **2010**, *20*, 1350–1371.

569 Clark, G.M. Changes in Patterns of Streamflow From Unregulated Watersheds in Idaho, Western
570 Wyoming, and Northern Nevada 1. *JAWRA Journal of the American Water Resources Association*
571 **2010**, *46*, 486–497.

572 Kunkel, K.E. Temporal variations in frost-free season in the United States: 1895–2000. *Geophysical*
573 *Research Letters* **2004**, *31*, 399.

574 Kormos, P.R.; Luce, C.H.; Wenger, S.J.; Berghuijs, W.R. Trends and sensitivities of low streamflow
575 extremes to discharge timing and magnitude in Pacific Northwest mountain streams. *Water*
576 *Resources Research* **2016**, *52*, 4990–5007.

577 Stillwater, L. The Effects of Climate Change on the Operation of Boise River Reservoirs, Initial
578 Assessment Report. *United States Bureau of Reclamation, Department of the Interior, Boise, Idaho*
579 **2008**.

580 Taylor, K.E.; Stouffer, R.J.; Meehl, G.A. An Overview of CMIP5 and the Experiment Design. *Bul-*
581 *letin of the American Meteorological Society* **2012**, *93*, 485–498.

582 Bolte, J.P.; Hulse, D.W.; Gregory, S.V.; Smith, C. Modeling biocomplexity – actors, landscapes and
583 alternative futures. *Environmental Modelling & Software* **2007**, *22*, 570–579.

584 Wu, H.; Bolte, J.P.; Hulse, D.; Johnson, B.R. A scenario-based approach to integrating flow-ecology
585 research with watershed development planning. *Geodesign—Changing the world, changing design*
586 **2015**, *144*, 74–89.

587 Turner, D.P.; Conklin, D.R.; Bolte, J.P. Projected climate change impacts on forest land cover and
588 land use over the Willamette River Basin, Oregon, USA. *Climatic Change* **2015**, *133*, 335–348.

589 Hulse, D.; Branscomb, A.; Enright, C.; Johnson, B.; Evers, C.; Bolte, J.; Ager, A. Anticipating
590 surprise: Using agent-based alternative futures simulation modeling to identify and map sur-

591 prising fires in the Willamette Valley, Oregon USA. *Geodesign—Changing the world, changing*
592 *design* **2016**, *156*, 26–43.

593 Han, B.; Benner, S.G.; Bolte, J.P.; Vache, K.B.; Flores, A.N. Coupling biophysical processes and
594 water rights to simulate spatially distributed water use in an intensively managed hydrologic
595 system. *Hydrology and Earth System Sciences* **2017**, *21*, 3671–3685.

596 Turner, D.P.; Conklin, D.R.; Vache, K.B.; Schwartz, C.; Nolin, A.W.; Chang, H.; Watson, E.; Bolte,
597 J.P. Assessing mechanisms of climate change impact on the upland forest water balance of the
598 Willamette River Basin, Oregon. *Ecohydrology* **2016**, *10*, e1776.

599 Bergström, S. Development and Application of a Conceptual Runoff Model for Scandinavian
600 Catchments. Technical Report RH07, Norrköping, 1976.

601 Seibert, J. Multi-criteria calibration of a conceptual runoff model using a genetic algorithm. *Hy-*
602 *drology and Earth System Sciences* **2000**, *4*, 215–224.

603 Woodsmith, R.; Vache, K.; McDonnell, J.; Seibert, J.; Helvey, J. The Entiat Experimental Forest: A
604 unique opportunity to examine hydrologic response to wildfire. Advancing the Fundamental
605 Sciences: Proceedings of the Forest Service National Earth Sciences Conference. M. Furniss, C.
606 Clifton, & K. Ronnenbery (editors). USDA, Forest Service, Portland, OR. PNW-GTR-689. Cite-
607 seer, 2007, pp. 205–216.

608 Abebe, N.A.; Ogden, F.L.; Pradhan, N.R. Sensitivity and uncertainty analysis of the conceptual
609 HBV rainfall–runoff model: Implications for parameter estimation. *Journal of Hydrology* **2010**,
610 *389*, 301–310.

611 Bergström, S.; Lindström, G. Interpretation of runoff processes in hydrological modelling-
612 experience from the HBV approach. *Hydrological Processes* **2015**, *29*, 3535–3545.

613 Seibert, J. Regionalisation of parameters for a conceptual rainfall-runoff model. *Agricultural and*
614 *Forest Meteorology* **1999**, *98-99*, 279–293.

615 Allen, R.G.; Pereira, L.S.; Raes, D.; Smith, M. Crop evapotranspiration - Guidelines for computing
616 crop water requirements. Technical Report 56, FAO Irrigation and Drainage Paper, 1998.

617 Allen, R.G.; Robison, C.W. Evapotranspiration and consumptive irrigation water requirements
618 for Idaho. *Precipitation Deficit Table for Boise WSFO Airport* **2007**.

619 Inouye, A.M. Development of a hydrologic model to explore impacts of climate change on water
620 resources in the Big Wood Basin, Idaho. Master's thesis, Oregon State University, 2014.

621 Abatzoglou, J.T.; Brown, T.J. A comparison of statistical downscaling methods suited for wildfire
622 applications. *International Journal of Climatology* **2011**, *32*, 772–780.

623 van Vuuren, D.P.; Edmonds, J.; Kainuma, M.; Riahi, K.; Thomson, A.; Hibbard, K.; Hurtt, G.C.;
624 Kram, T.; Krey, V.; Lamarque, J.F.; Masui, T.; Meinshausen, M.; Nakicenovic, N.; Smith, S.J.;
625 Rose, S.K. The representative concentration pathways: an overview. *Climatic Change* **2011**,
626 *109*, 5.

627 Rupp, D.E.; Abatzoglou, J.T.; Hegewisch, K.C.; Mote, P.W. Evaluation of CMIP5 20th century
628 climate simulations for the Pacific Northwest USA. *Journal of Geophysical Research: Atmospheres*
629 **2013**, *118*, 10,884–10,906.

630 Abatzoglou, J.T. Development of gridded surface meteorological data for ecological applications
631 and modelling. *International Journal of Climatology* **2011**, *33*, 121–131.

632 Mitchell, K.E. The multi-institution North American Land Data Assimilation System (NLDAS):
633 Utilizing multiple GCIP products and partners in a continental distributed hydrological mod-
634 eling system. *Journal of Geophysical Research* **2004**, *109*, 7449.

635 Beven, K. A manifesto for the equifinality thesis. *Journal of Hydrology* **2006**, *320*, 18–36.

636 Gupta, H.V.; Beven, K.J.; Wagener, T. Model calibration and uncertainty estimation. *Encyclopedia*
637 *of hydrological sciences* **2005**.

638 Madsen, H. Parameter estimation in distributed hydrological catchment modelling using auto-
639 matic calibration with multiple objectives. *Snow–Atmosphere Interactions and Hydrological Conse-*
640 *quences* **2003**, *26*, 205–216.

641 Seibert, J. Estimation of Parameter Uncertainty in the HBV Model: Paper presented at the Nordic
642 Hydrological Conference (Akureyri, Iceland-August 1996). *Hydrology Research* **1997**, *28*, 247–262.

643 Hope, A.; Peck, E.L. Soil Moisture Release Data (FIFE). *ORNL DAAC, Oak Ridge, Tennessee, USA*
644 **1994**.

645 Nash, J.E.; Sutcliffe, J.V. River flow forecasting through conceptual models part I — A discussion
646 of principles. *Journal of Hydrology* **1970**, *10*, 282–290.

647 Moriasi, D.N.; Arnold, J.G.; Van Liew, M.W.; Bingner, R.L.; Harmel, R.D.; Veith, T.L. Model Evalu-
648 ation Guidelines for Systematic Quantification of Accuracy in Watershed Simulations. *Trans. of*
649 *the ASABE* **2007**, *50*, 885.

650 Krause, P.; Boyle, D.P.; Bäse, F. Comparison of different efficiency criteria for hydrological model
651 assessment. *Advances in Geosciences* **2005**, *5*, 89–97.

652 Steimke, A.; Flores, A.; Han, B.; Brandt, J.; Som-Castellano, R. Modeled impacts of climate change
653 on regional hydrology in the Upper Boise River Basin, Idaho, 2017.

654 Stewart, I.T.; Cayan, D.R.; Dettinger, M.D. Changes toward Earlier Streamflow Timing across
655 Western North America. *Journal of Climate* **2005**, *18*, 1136–1155.

656 Bohr, G.S.; Aguado, E. Use of April 1 SWE measurements as estimates of peak seasonal snowpack
657 and total cold-season precipitation. *Water Resources Research* **2001**, *37*, 51–60.

658 Garst, R.D. Using Mountain Snowpack to Predict Summer Water Availability in Semiarid Moun-
659 tain Watersheds. Master’s thesis, Boise State University, 2017.

- 660 Pederson, G.T.; Gray, S.T.; Woodhouse, C.A.; Betancourt, J.L.; Fagre, D.B.; Littell, J.S.; Watson, E.;
661 Luckman, B.H.; Graumlich, L.J. The Unusual Nature of Recent Snowpack Declines in the North
662 American Cordillera. *Science* **2011**, *333*, 332–335.
- 663 Klos, P.Z.; Link, T.E.; Abatzoglou, J.T. Extent of the rain-snow transition zone in the western U.S.
664 under historic and projected climate. *Geophysical Research Letters* **2014**, *41*, 4560–4568.
- 665 Dahal, K.R.; Benner, S.; Lindquist, E. Urban hypotheses and spatiotemporal characterization of
666 urban growth in the Treasure Valley of Idaho, USA. *Applied Geography* **2017**, *79*, 11–25.

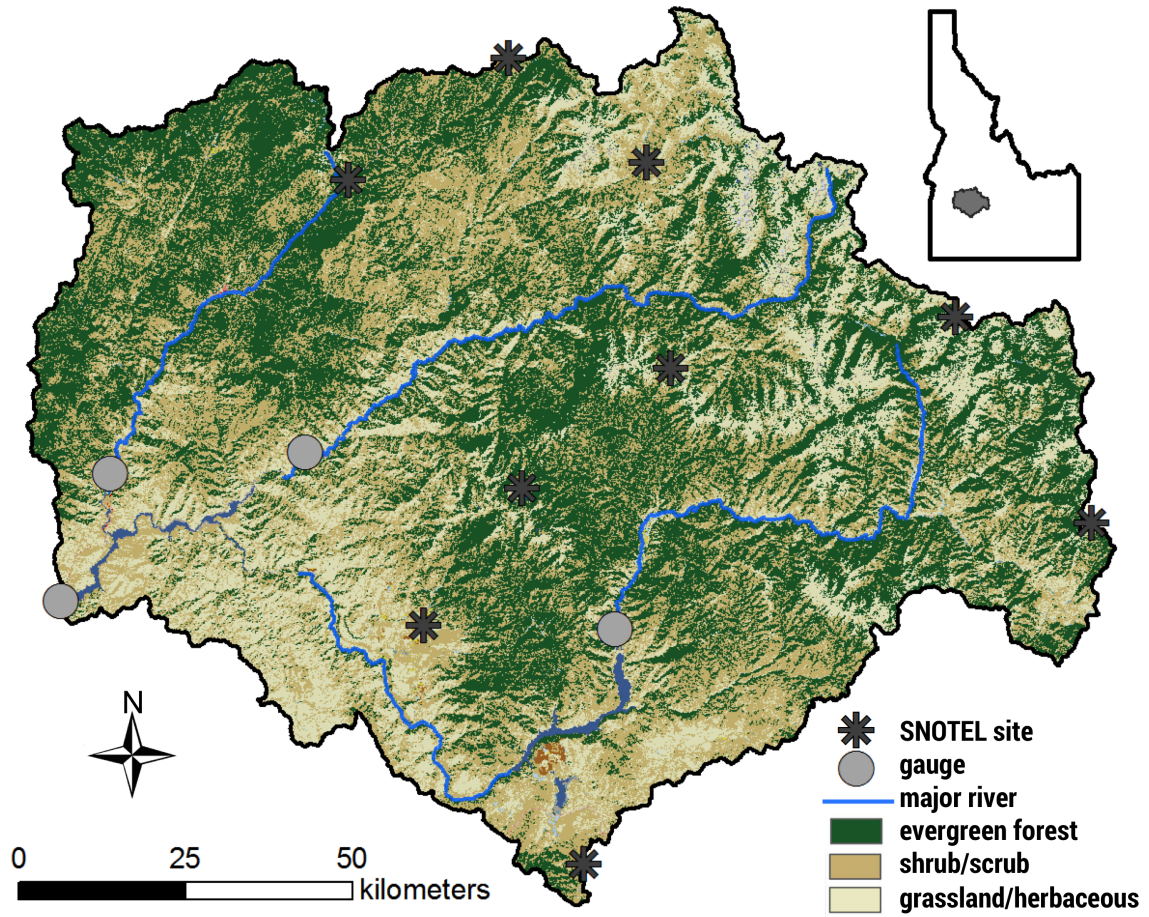


Figure 1: Overview of the study area with major land cover types and locations of SNOTEL stations and gauge locations (see Table 5 for names of gauges).

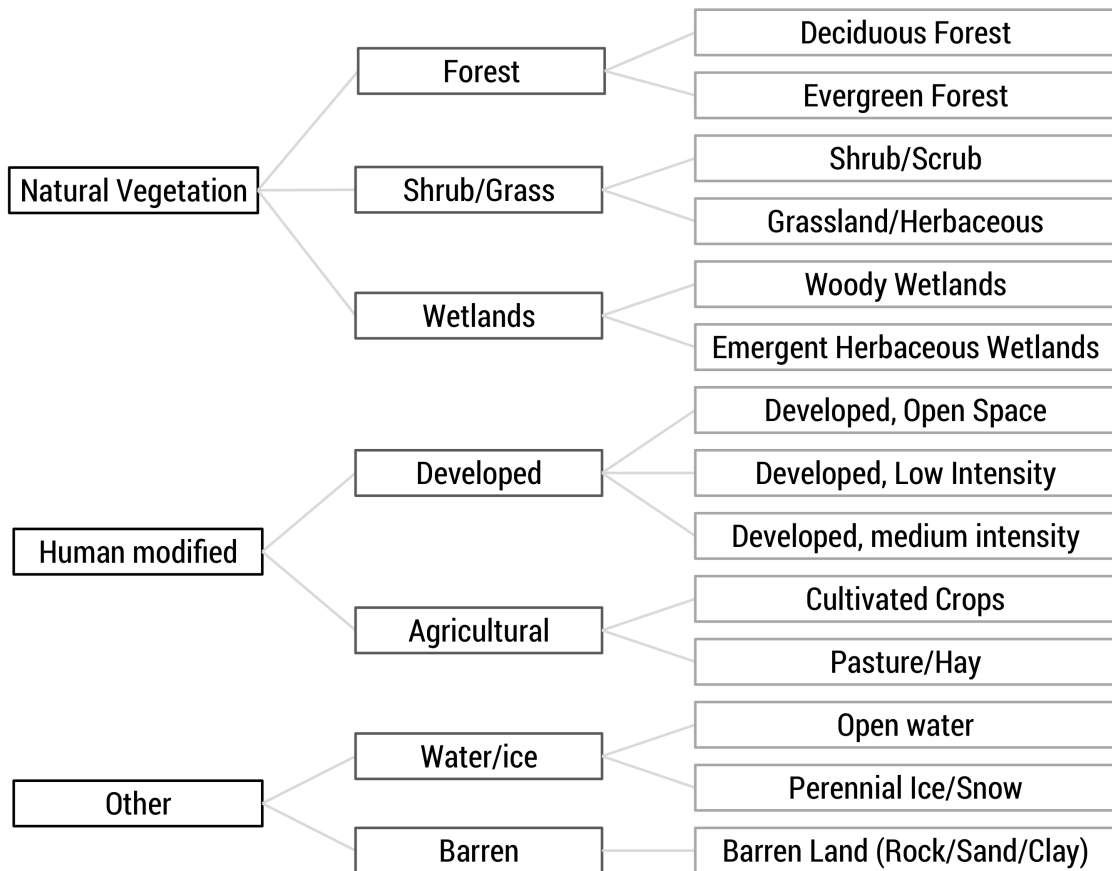


Figure 2: Land use/land cover tree developed for Envision. The tree allows for modeling algorithms to be applied at different hierarchy levels, from more general to more specific land types. The finest categories on the right correspond to the NLCD land classification system.

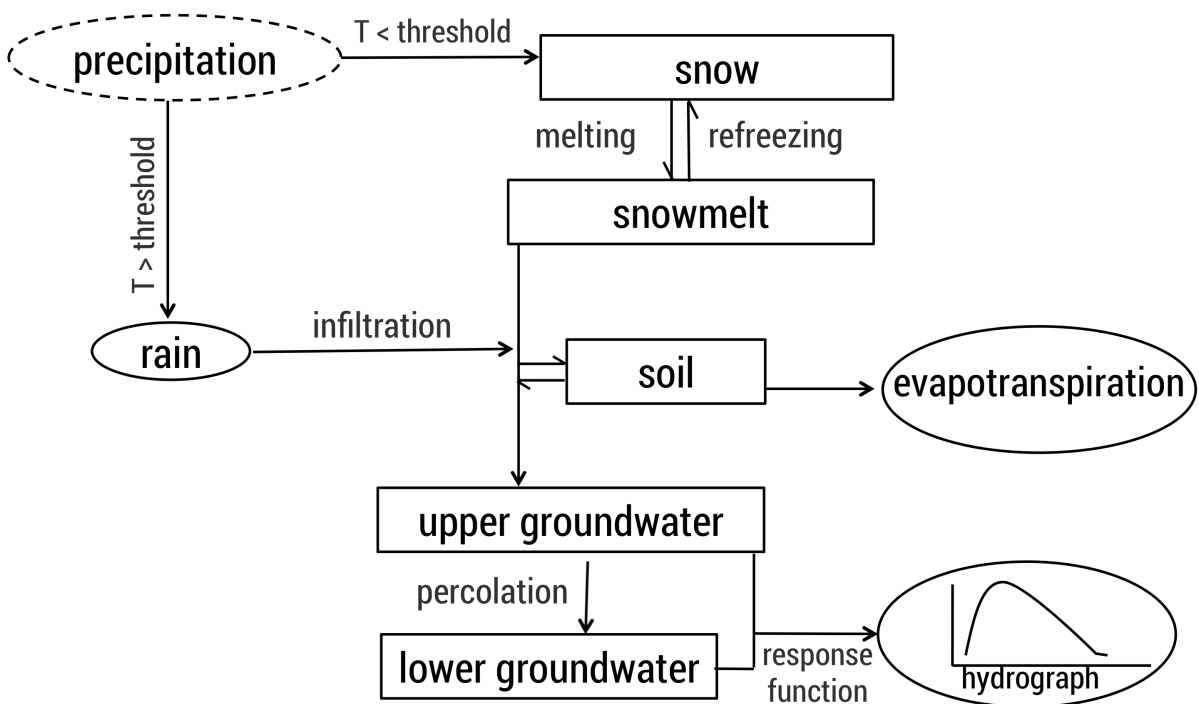


Figure 3: Flowchart of the different hydrologic processes and reservoirs within the Flow model in Envision, (modified from Han *et al.*, 2017)

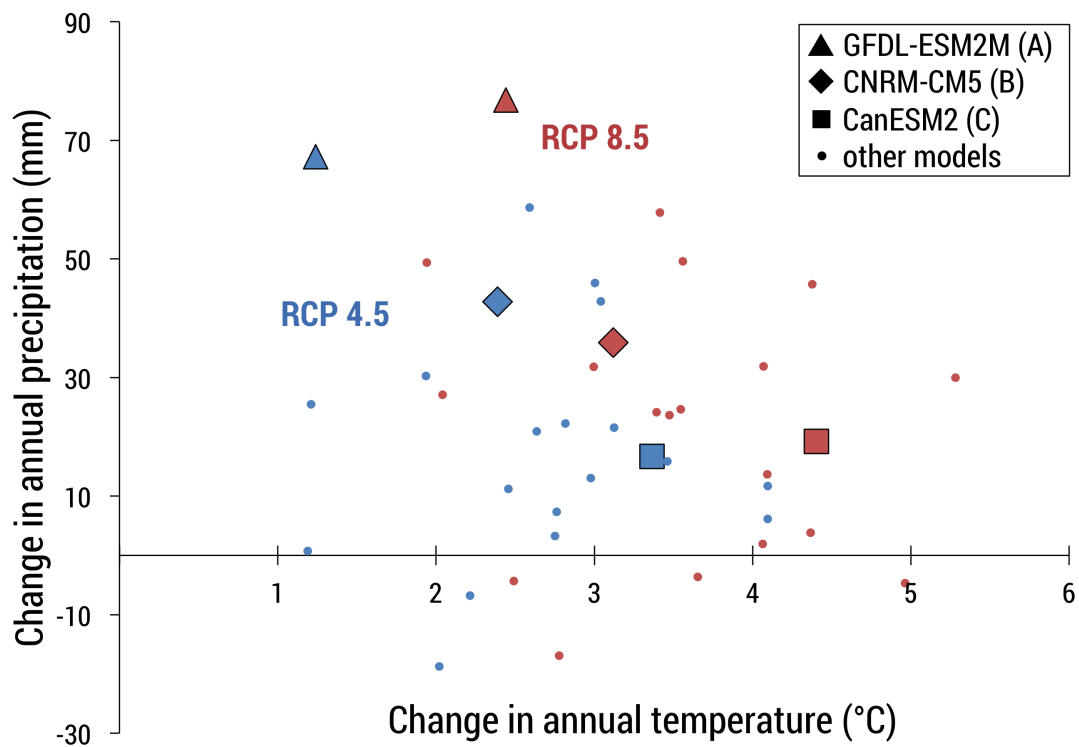


Figure 4: Change in climate variables from 1979-2000 to 2040-2069 for MACA downscaled GCMs (Abatzoglou and Brown, 2011). Blue and red points represent RCP 4.5 and 8.5 scenarios, respectively. The larger icons represent the GCMs selected for this study.

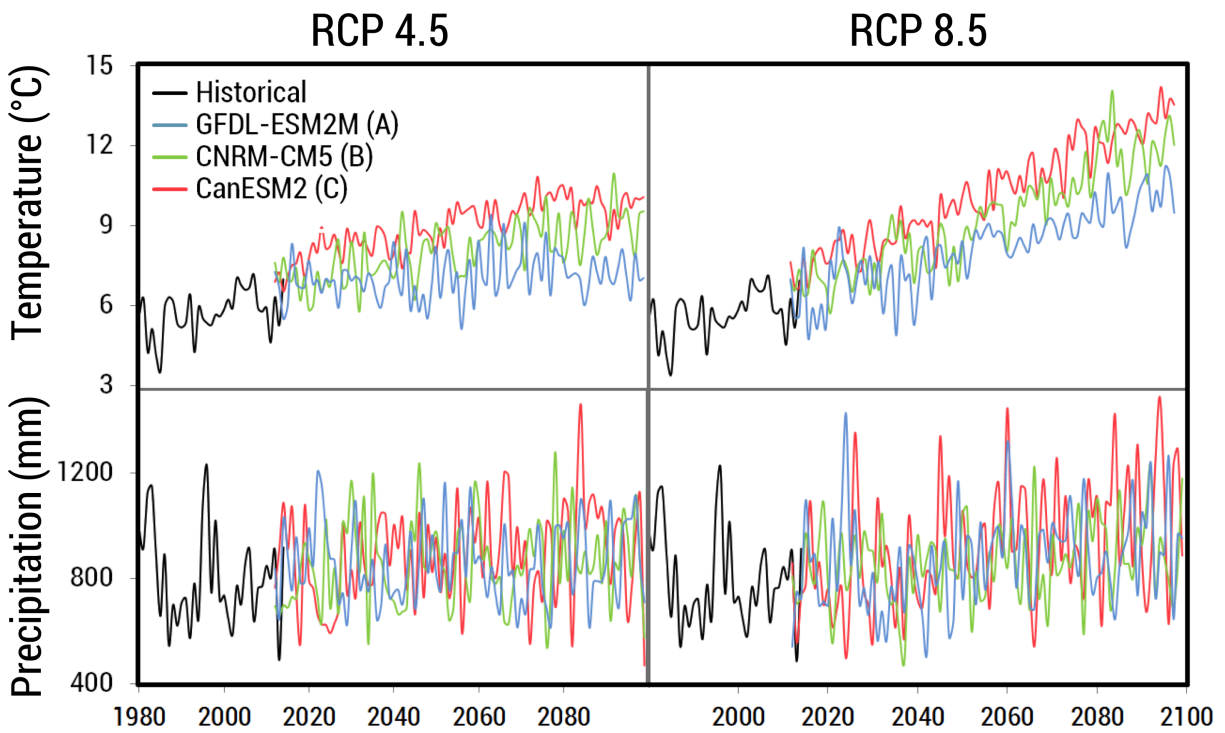


Figure 5: Temporal projections for annual mean temperature and precipitation for the six climate scenarios used in this study. Temperature increases in all scenarios, but precipitation is more variable.

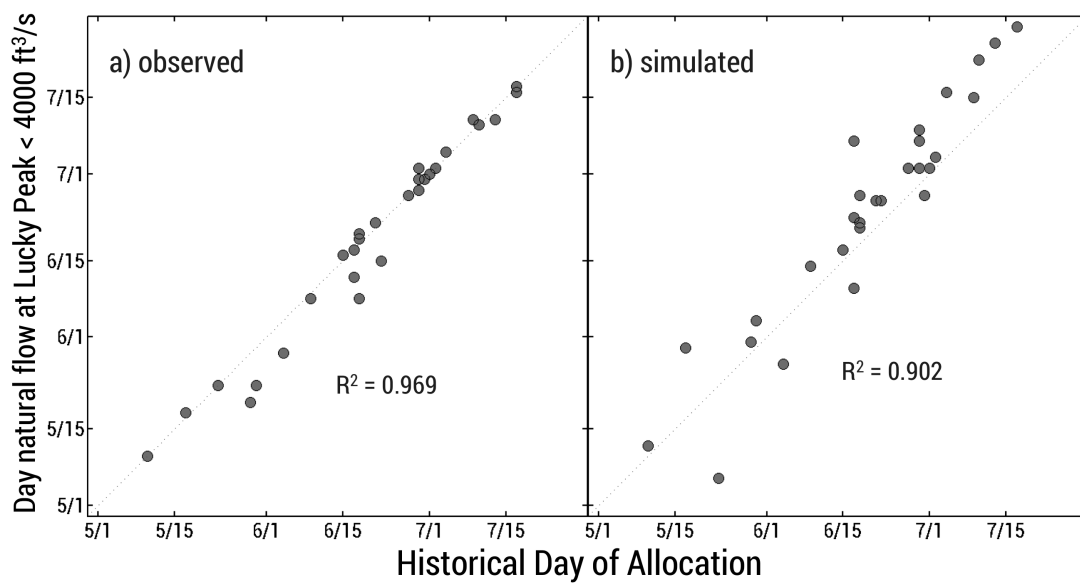


Figure 6: (a) Relationship between the day natural flow at Lucky Peak reaches below 4000 ft³/s and the date the Day of Allocation is declared, modified from (Garst, 2017). (b) Our modeled historical Day of Allocation using the same method as (a). Dashed line is 1:1 in both plots.

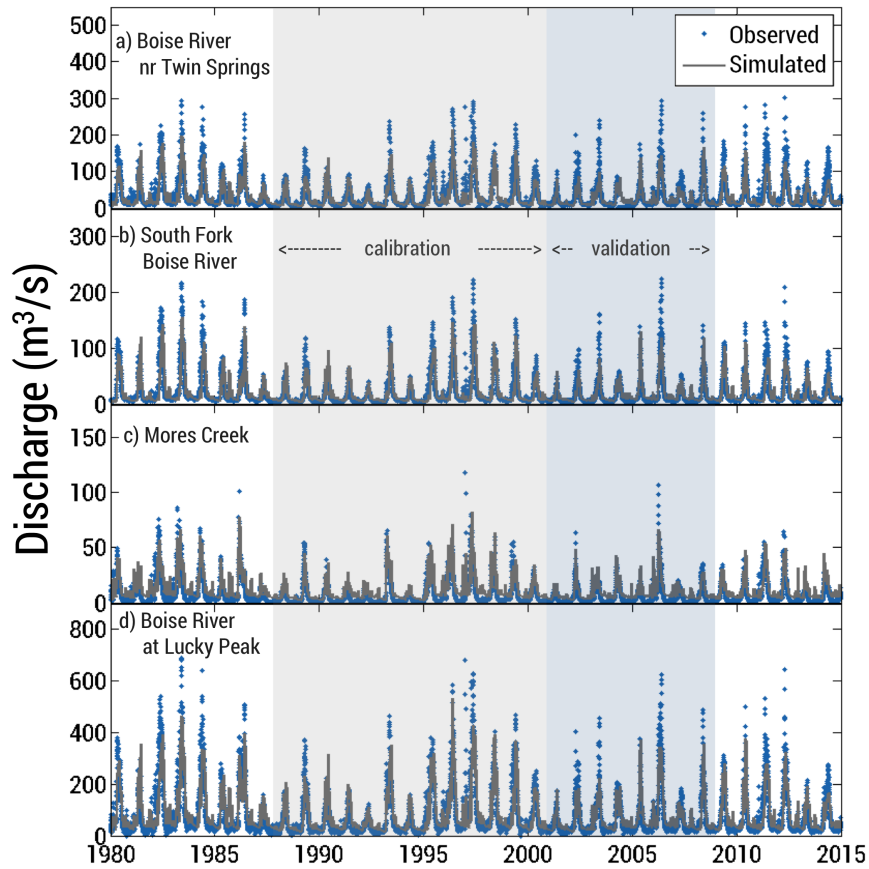


Figure 7: Observed and simulated streamflows during the historical period from 1980 to 2014. See Figure 1 for locations of sites. The model does a good job at simulating historical flows, but under estimates magnitude of peak flows and over estimates baseflow at Mores Creek.

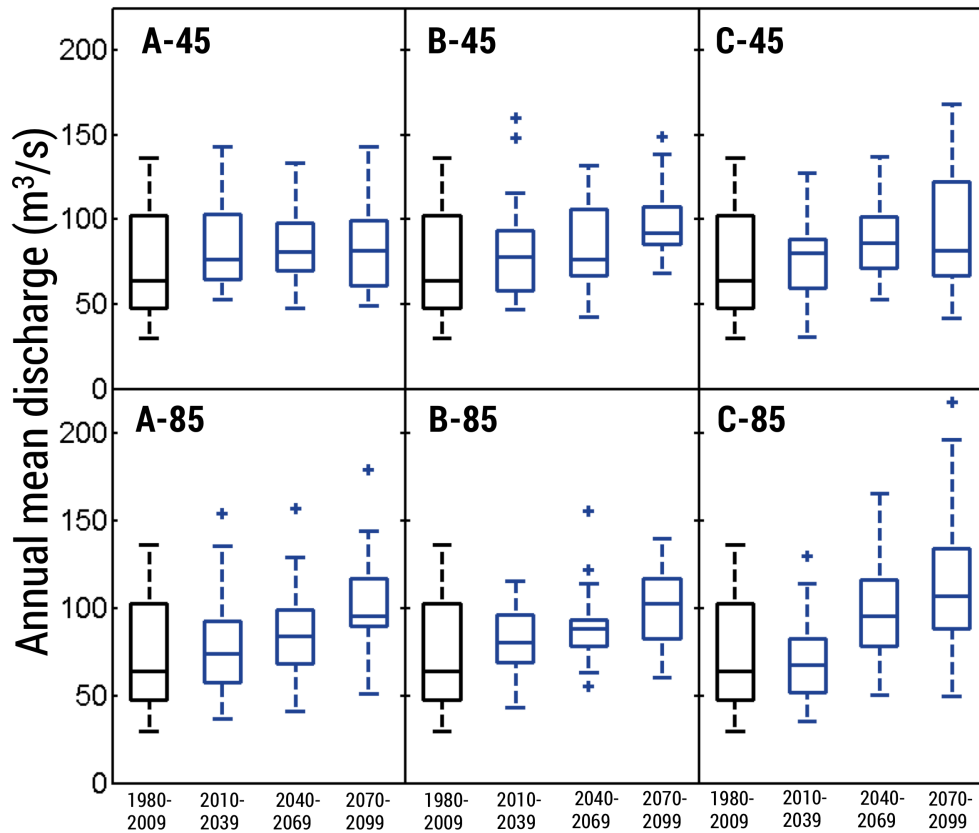


Figure 8: Average annual discharge of the UBRB. Values for 1980-2009 are observed. In most scenarios, we see an increase in overall discharge throughout the century. Boxes represent upper and lower quartiles and lines inside are the median.

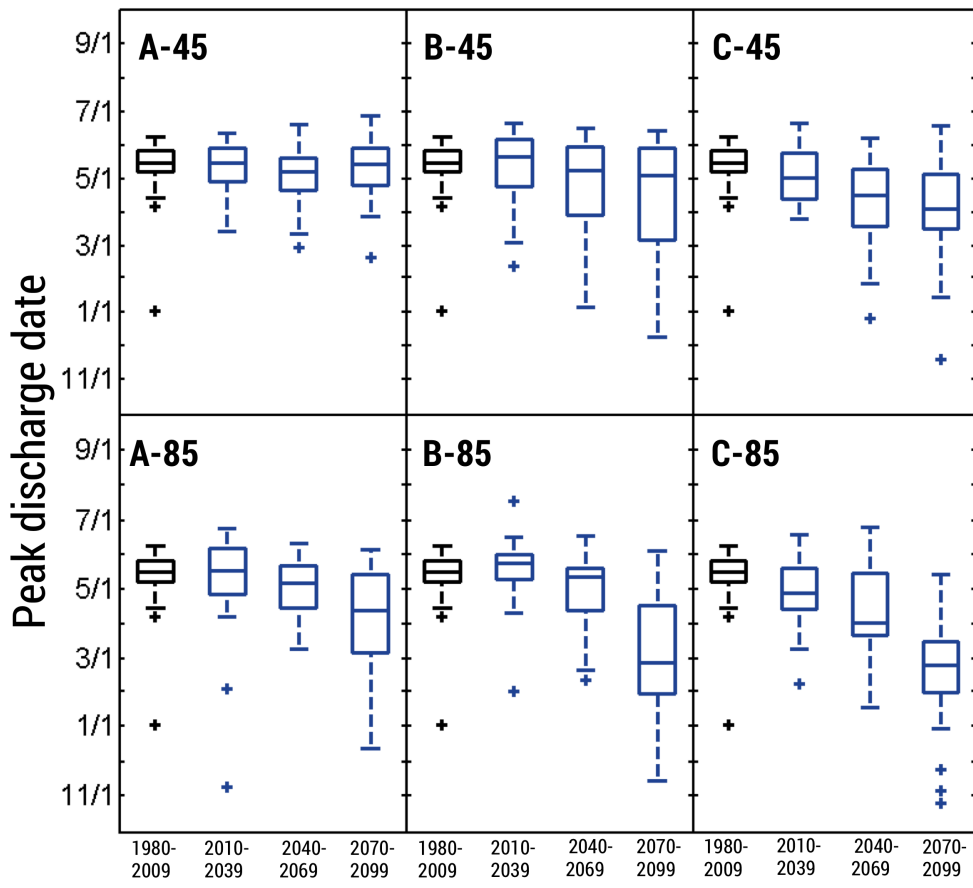


Figure 9: Date when peak discharge occurs for the Boise River at Lucky Peak. Values for 1980-2009 are observed. Overall, we see peak discharge date moving substantially earlier in five scenarios.

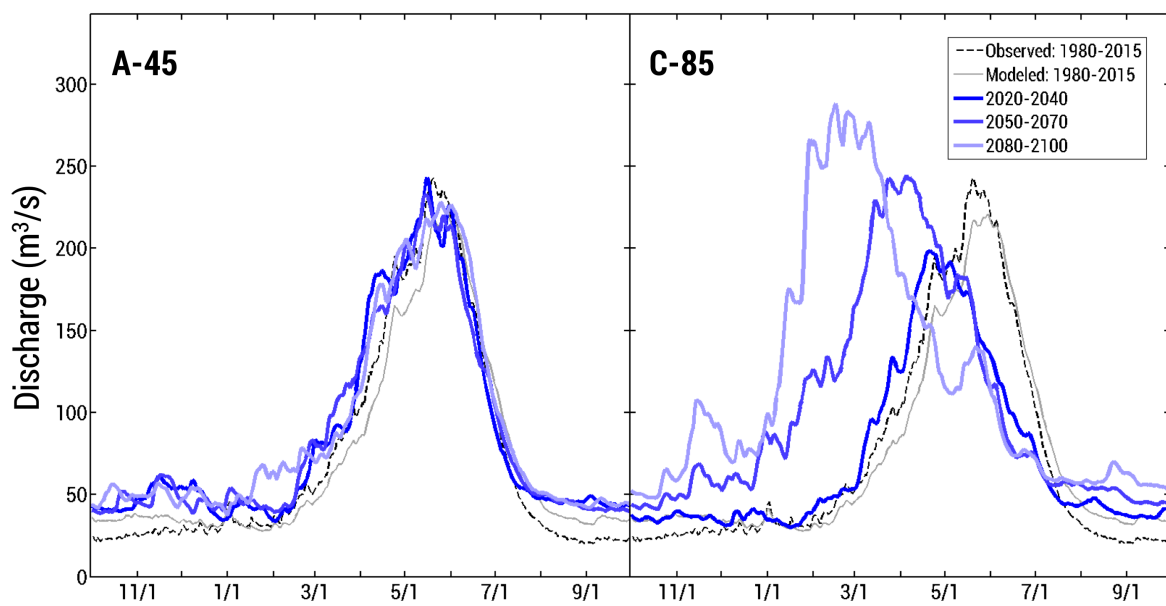


Figure 10: Hydrographs averaged over 2-decadal timespans for scenarios predicting the least amount of change (A-45) and the greatest amount of change (C-85) from historical.

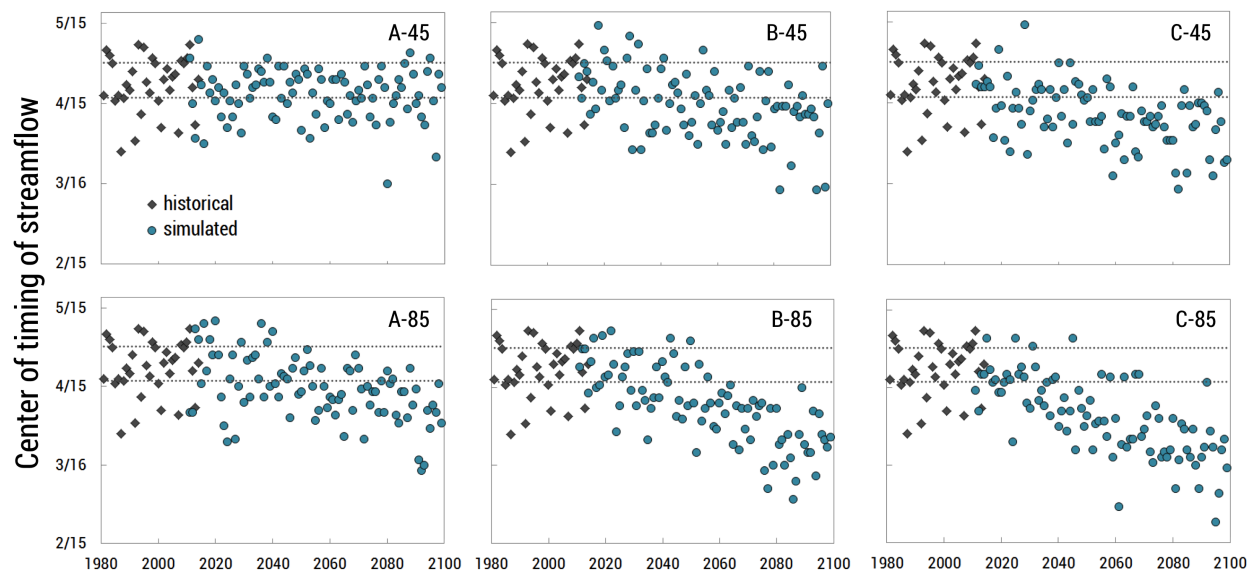


Figure 11: Center of timing of streamflow for historic and future simulations. Dashed lines show the upper and lower quartile ranges from 1980-2009.

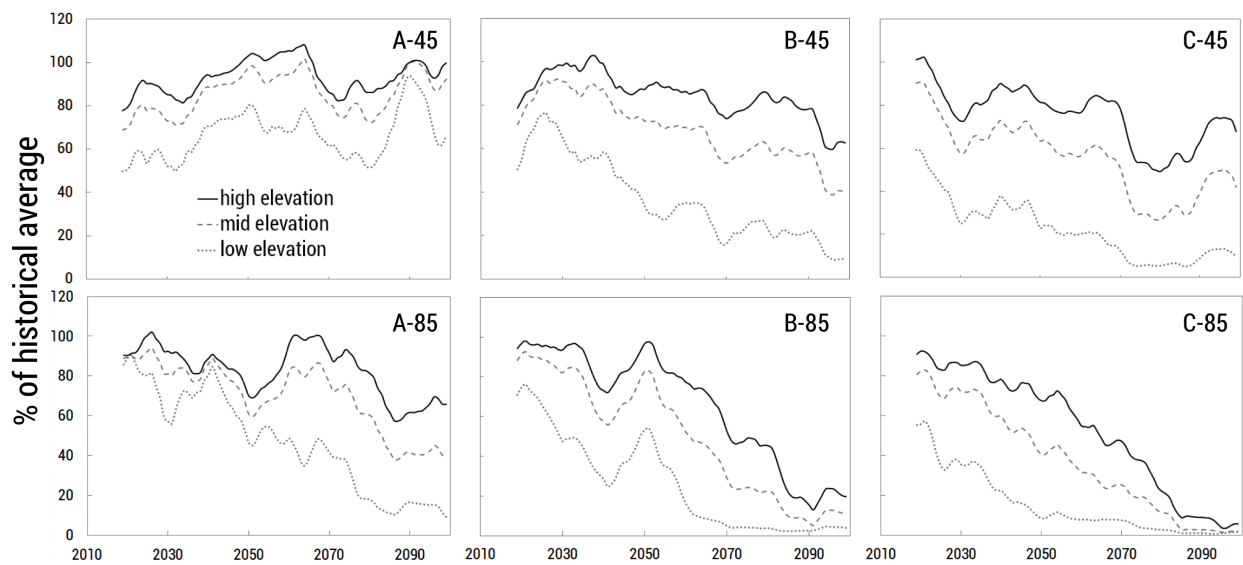


Figure 12: 10-year moving average percentage of April 1 SWE from historical simulated averages (1980-2009) for low, medium, and high elevation zones, corresponding to 1500-2000, 2000-2500, and 2500+ m, respectively.

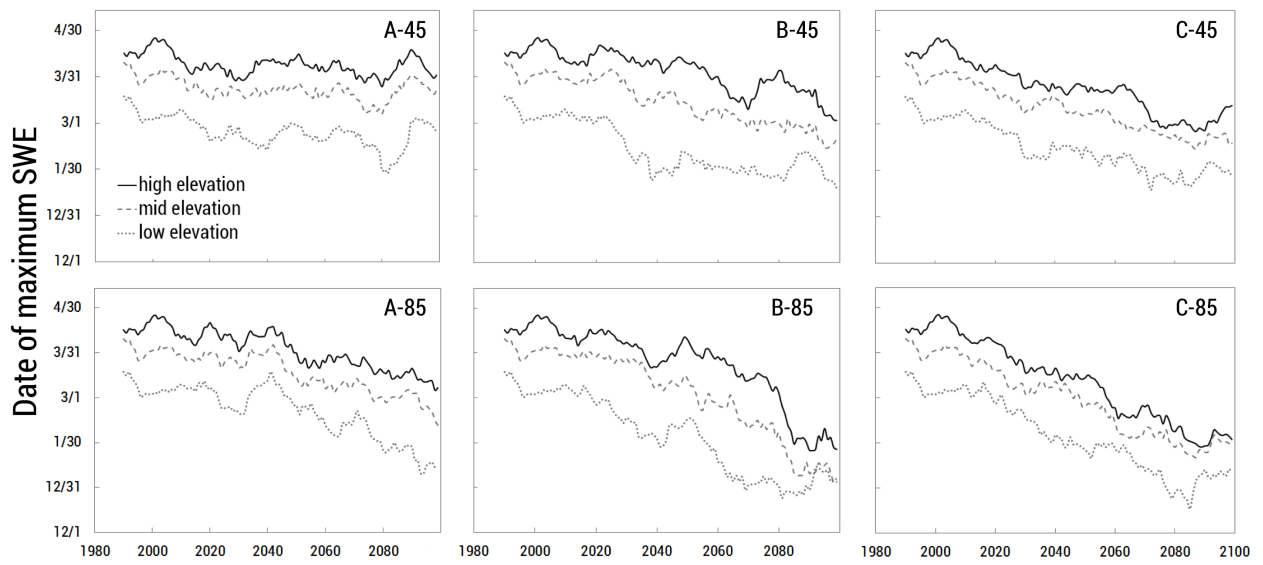


Figure 13: 10-year moving average of dates of maximum SWE for three elevation zones. Values for 1980-2009 are simulated with MACA METDATA.

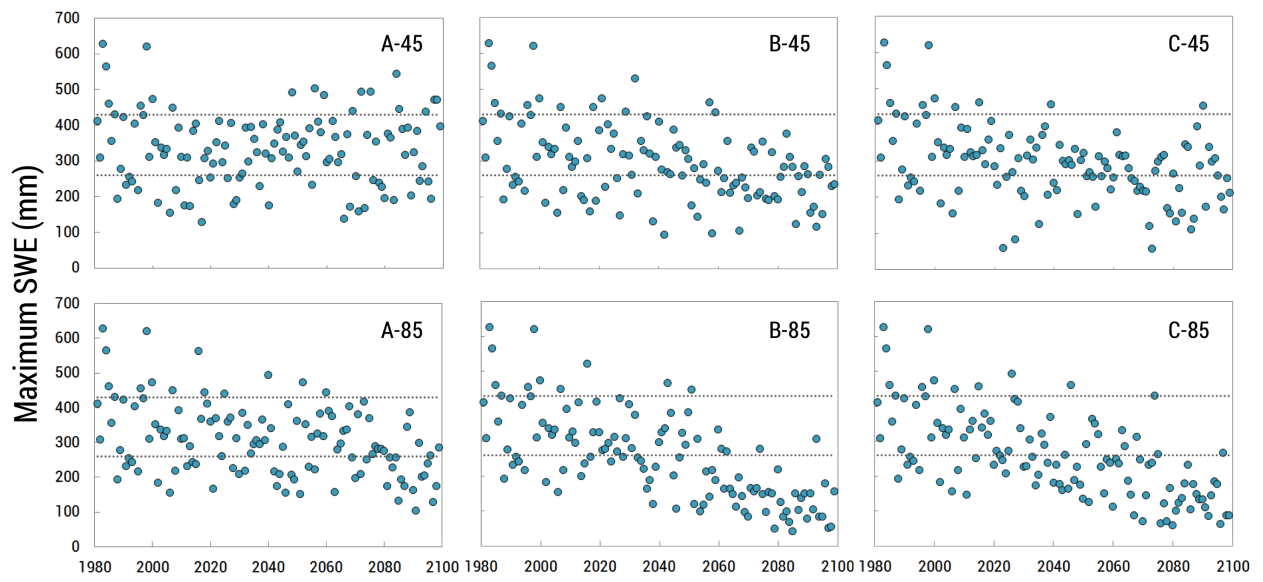


Figure 14: Maximum SWE amount (mm) for mid-elevations (2000-2500 m). Values for 1980-2009 are simulated with MACA METDATA. Dashed lines show upper and lower quartile ranges for 1980-2009.

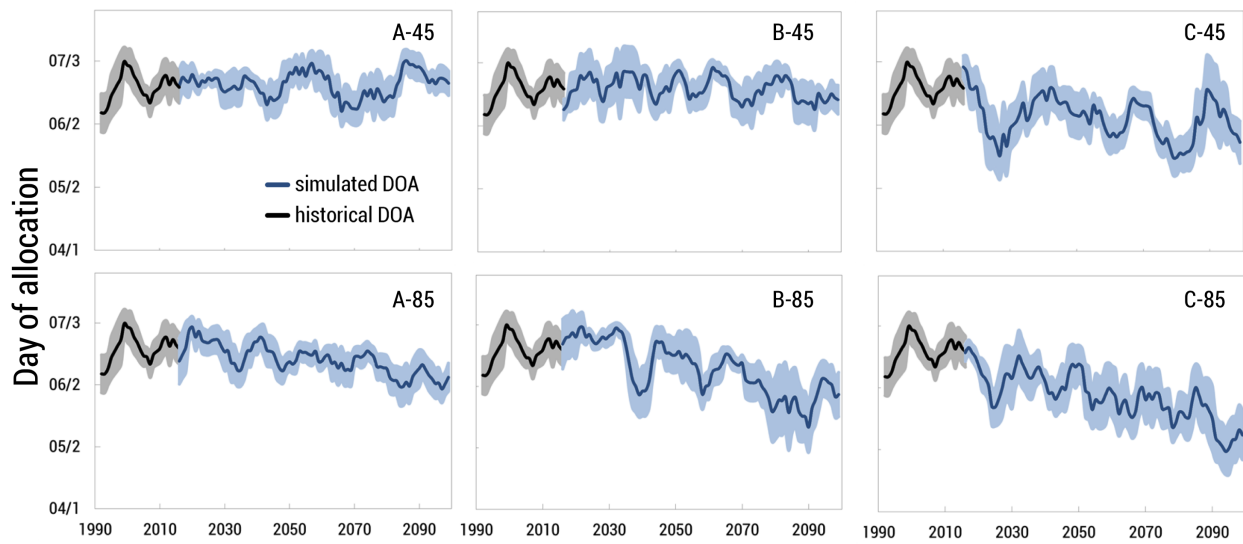


Figure 15: Simulated future (2010-2099) and historical (1986-2014) Day of Allocation with a 7-year moving average. Shaded area is $\pm 0.5\sigma$ of 7-year moving average values.

Table 1: Data sources used for spatial coverage in Envision

Input Data (<i>resolution</i>)	Data Sources	Used In
Surface Management Agency	Bureau of Land Management	IDU
Land Cover (30 m)	National Landcover Database (2011)	IDU, ET
Streams & Catchments (HUC12)	NHD Plus V2	IDU, HBV
Elevation (30 m)	National Elevation Dataset	HRU

Table 2: Land cover type in Envision and the associated crop used to calculate evapotranspiration

Land Cover	Crop substituted for land cover	Source
Forest	3 rd year poplar \times 3	Agrimet, Inouye (2014)
Shrubland	Sagebrush	Allen and Robison (2007)
Grassland	Bunch grass	Allen and Robison (2007)
Wetlands	Poplar \times 3	Agrimet, Inouye (2014)
Developed	Lawn \times 0.21	Agrimet, Inouye (2014)
Agricultural	Alfalfa (mean)	Agrimet

Table 3: Naming convention for the six climate scenarios used in this study

	GFDL-ESM2M (warm)	CNRM-CM5 (warmer)	CanESM2 (warmest)
RCP4.5	A-45	B-45	C-45
RCP8.5	A-85	B-85	C-85

Table 4: Parameters for Flow and the ranges/values considered for calibration

Routine	Parameter	Description	Units	Range	Value
Snow Routine	TT	Threshold temperature	°C	-0.5 – 2.0	1.335
	CFMAX	Degree-day factor	mm°C ⁻¹ day ⁻¹	1.0 – 6.0	1.489
	SFCF	Snowfall correction factor	-	0.7 – 1.2	0.568
	CFR	Refreeze coefficient	-	-	0.05
	CWH	Water holding capacity of snowpack	-	-	0.1
Soil and Evaporation Routine	FC*	Max depth of water in soil water reservoir	mm	-	399.7
	LP*	Soil moisture value where actual ET=PET	mm	-	247.2
	WP*	Wilting point in soil for ET to occur	mm	-	156.2
	BETA	Shaping coefficient	-	1.0 – 6.0	2.015
	PERC	Percolation coefficient	day ⁻¹	0.1 – 2.0	1.272
Groundwater and Response Routine	UZL	Threshold for K0 to outflow	mm	1.0 – 400.0	365.4
	K0	Recession coefficient	day ⁻¹	0.1 – 1.0	0.339
	K1	Recession coefficient	day ⁻¹	0.01 – 0.5	0.079
	K2	Recession coefficient	day ⁻¹	0.001 – 0.15	0.004

* values obtained from ORNL DAAC SDAT

Table 5: Data sites used for calibration and validation. See Figure 1 for locations of gauges.

Type	Name	Drainage Area (km ²)	Record Length	Site ID
Gauge	a) Boise River nr Twin Springs	2154.9	1911 – present	13185000
	b) SF Boise River nr Featherville	1660.2	1945 – present	13186000
	c) Mores Creek abv Robie Creek	1028.2	1950 – present	13200000
	d) Boise River at Lucky Peak*	6571	1895 – present	LUC
Type	Name	Elevation (m)	Record Length	Site ID
SNOTEL	Atlanta Summit	2310	1981 – present	306
	Camas Creek	1740	1992 – present	382
	Dollarhide Summit	2566	1981 – present	450
	Graham Guard Station	1734	1981 – present	496
	Jackson Peak	2155	1981 – present	550
	Mores Creek	1859	1981 – present	637
	Prairie	1463	1987 – present	704
	Trinity	2368	1981 – present	830
	Vienna Mine	2731	1979 – present	845

*not an actual gauge, but a calculated daily average of runoff at this location if dams were not present. Obtained from the US Bureau of Reclamation.

Table 6: Calibration and validation results for the chosen parameter set for this study.

Calibration					Validation				
NSE_G	$\log NSE_G$	VE_G	NSE_S	$Obj.$	NSE_G	$\log NSE_G$	VE_G	NSE_S	$Obj.$
0.71	0.61	-0.03	0.59	0.63	0.70	0.66	-0.06	0.52	0.62

Table 7: Simulated mean Day of Allocation (DOA) and standard deviation (*italicized, in parentheses*) over three future time intervals. Historical (1986-2014) average DOA is 6/19.

Time Period	A-45	B-45	C-45	A-85	B-85	C-85
2010-2039	6/22 (12.0)	6/21 (20.0)	6/10 (24.3)	6/19 (17.1)	6/20 (20.6)	6/10 (19.0)
2040-2069	6/20 (17.3)	6/20 (15.3)	6/7 (16.8)	6/15 (13.1)	6/15 (17.2)	5/30 (23.5)
2070-2099	6/23 (15.1)	6/18 (16.1)	5/29 (24.0)	6/8 (14.9)	5/27 (25.6)	5/17 (23.5)